Article

Synthesis of Helical Analogue of Kekulene: a Flexible #-Expanded Helicene with Large Helical Diameter Acting as a Soft Molecular Spring

Yusuke Nakakuki, Takashi Hirose, and Kenji Matsuda

J. Am. Chem. Soc., **Just Accepted Manuscript** • DOI: 10.1021/jacs.8b09825 • Publication Date (Web): 19 Oct 2018

Synthesis of Helical Analogue of Kekulene: a Flexible π-Expanded Helicene with Large Helical Diameter Acting as a Soft Molecular Spring

Yusuke Nakakuki, Takashi Hirose, and Kenji Matsuda**

Department of Synthetic Chemistry and Biological Chemistry, Graduate School of Engineering, Kyoto University, Katsura, Nishikyo-ku, Kyoto 615-8510, Japan.

*e-mail: thirose@sbchem.kyoto-u.ac.jp (T.H.), kmatsuda@sbchem.kyoto-u.ac.jp (K.M.)

Abstract: A π-expanded helicene, that is the helically twisted analogue of kekulene, was synthesized using a 6-fold ring-closing olefin metathesis (RCM) reaction as a key step. The π-expanded geometry with large helical diameter (d_h = 10.2 Å), consisting only of carbon and hydrogen atoms ($C_{54}H_{30}$), was unambiguously determined by single-crystal X-ray analysis. We found that the π-expanded helicene with large helical diameter will act as a soft molecular spring with a small spring constant. Interestingly, the mechanical properties of molecular springs roughly satisfied a physical formula for macroscopic spring materials, i.e., the force constant of the elongation of molecular spring (k) is inversely proportional to the third power of the helical diameter ($k \propto d_h^{-3}$).

Introduction

Synthesis of chiral compounds is one of the main concerns in chemistry to elucidate their unique properties.[1–4] Helicenes—*ortho*-fused polycyclic aromatic hydrocarbons (PAHs)—are representative examples of helically twisted molecules,[5] which have been widely investigated from the viewpoint of challenging targets of (asymmetric) organic synthesis[6–9] as well as the viewpoint of chiral organic materials showing remarkable response to circularly polarized light[10–13] and large nonlinear optical (NLO) properties.[14–16] Following the recent advances in organic chemistry to construct highly strained molecules,[17–20] impressive π-extended helicenes have been reported in the last five years, including pyrene-based π-extended helicenes by Collins[21] and by Sterá and Starý,[22,23] perylene bisimide-based π-conjugated helices by Nuckolls,[24,25] and double and multiple-pole helicenes consisting of two or more helicene-like subunits by Itami,[26,27] Müllen,[28,29] Kamikawa,[30] Coquerel and Gingras,[31] and Wang.[32]

By making planar PAHs nonplanar, a number of basic structures of helically twisted molecules can be systematically designed. From this perspective, [7]helicene ($C_{30}H_{18}$) can be regarded as the helical analogue of coronene, which is the smallest helical PAHs with helical diameter (d_h) of 5.1 Å, where d_h is defined by the longest distance between the centroids of polycyclic rings (Figure 1). Recently, we have reported the synthesis of hexa-*peri*-

hexabenzo[7]helicene ($C_{48}H_{24}$),[33] which is the helical analogue of hexa-*peri*-hexabenzocoronene. The homogeneous π-extension throughout the helicene structure eventually leads to the helically twisted graphenes that can be considered as a promising candidate as a helix-shaped molecular element in molecular electronic devices.[34,35]

Besides the π-extension of helicenes, another molecular design strategy is the expansion of helicene framework, i.e., the increasing in helical diameter. With this approach, a number of basic molecular structures of helically twisted PAHs can be designed (Figure 1). One distinctive example of π-expanded helicenes is angularly fused helical phenylenes, so-called heliphenes.[36–38] The synthesis of [*n*]heliphenes (*n* = 5–9) has been achieved by Vollhardt et al. in 2002 using cobalt-catalyzed [2+2+2] cycloaddition of alkynes. Since the pioneering works by Vollhardt, the chemistry of π-expanded helicene has been largely undeveloped except for a few examples including indeno-fused helicenes by Wang in 2004,[39] oligonaphthofrans by Tsubaki in 2014,[40] and oxahelicenes by Vacek, Stará, and Starý in 2017.[41]

Kekulene is a π-expanded planar PAH consisting of hexagonally fused 12 benzene rings with D_{6h} symmetry (Figure 1). The synthesis of kekulene was reported for the first time by Diederich and Staab in 1978.[43,44] [7]Heliphene ($C_{42}H_{18}$) can be regarded as the helical analogue of anti-kekulene—a kekulene-like molecule showing an anti-aromatic character in which alternating

6 benzene rings of kekulene are replaced by 4-membered ring.[45,46] A chemical structure of the helical analogue of kekulene has been reported as "a conceptual molecule" by Bell in 1991.[47] Recently, Tilley et al. reported the synthesis of helically twisted analogue of kekulene using iridium-catalyzed [2+2+2] cycloaddition of alkynes in 2017.[42] The synthetic strategy proposed by Tilley is beneficial for affording a series of substituted π-expanded helicenes, however, the synthesis of the basic structure of helical analogue of kekulene, especially with no substituent group, has not been achieved for 40 years since the first report of kekulene.

In this work, we synthesized a π-expanded helicene **1** ($C_{54}H_{30}$), that is the basic structure of helically twisted analogue of kekulene, using Suzuki–Miyaura coupling and ring-closing metathesis reactions as the key steps (Figure 1). The synthesis of non-functionalized compounds is of importance to elucidate the origin of unique molecular properties derived from a primary molecular structure. For this purpose, the synthesis of the simplest chemical structures as a model compound is highly required. In the current study, we focused on the elucidation of the local aromaticity, photophysical properties, and molecular mechanical properties of the π-expanded helicenes. The π-expanded geometry with large helical diameter (d_h = 10.2 Å) was unambiguously determined by X-ray crystallography. Because of the larger helical diameter, the magnitude of transition magnetic dipole moment of **1** was roughly three times larger than that of [7]helicene.

We revealed that the π-expanded structure of **1** consisting solely of benzene rings is remarkably flexible even more than [7]heliphene. The flexibility of **1** is likely attributed to the π-expanded molecular framework with large helical diameter, consisting of many C–C bonds in a helical pitch, by which the steric distortion required for stretching and racemization of helix-shaped molecule can be effectively dispersed.

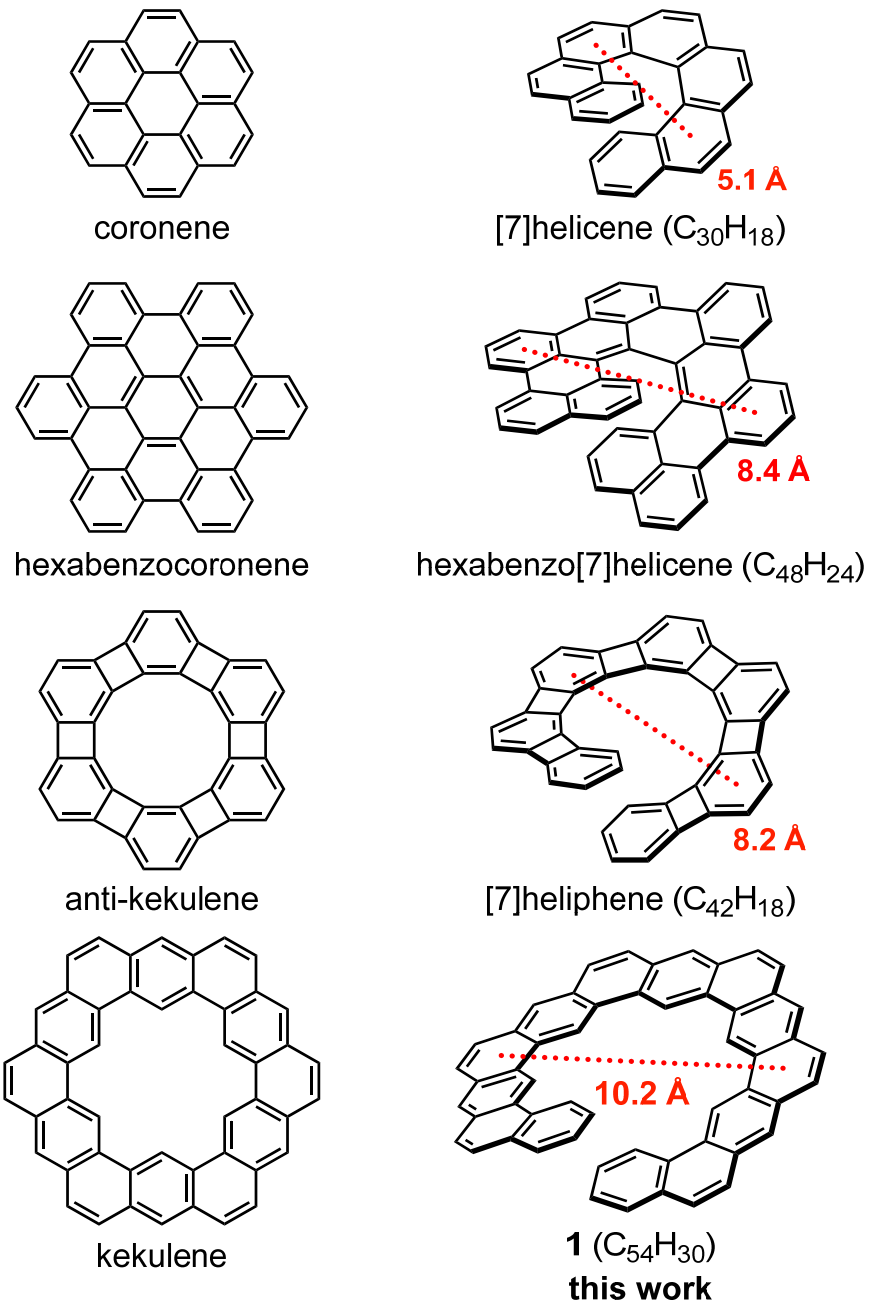

Figure 1. Chemical structure of planar (left) and helically twisted PAHs (right). Each helically twisted analogue can be systematically generated from a planar PAH by making an open-ring structure so that one benzene ring is duplicated. Helical diameters defined by the distance between the centroids of outer rings are shown in red.

Results and Discussion

Synthesis of Helical Analogue of Kekulene. The ring-closing olefin metathesis (RCM) reactions are a powerful approach for the formation of polycyclic structures.[48,49] Collins reported that the RCM reaction can be applicable to the synthesis of helicenes despite the structure of product is significantly strained.[50] The applicability of RCM reaction in the synthesis of complicated polycyclic systems has further underlined by King in the synthesis of septulene—a heptagonal analogue of kekulene consisting of 14 benzene rings.[51] In the present work, the synthesis of the helical analogue of kekulene **1** was performed in a stepwise fashion using Suzuki–Miyaura coupling to construct *m*-septiphenyl framework **9** and then using RCM reaction as the final step (Scheme 1). 1,5-Dibromo-2,4-bis(prop-1-enyl)benzene (**2**) was prepared from *m*-xylene by a two-step sequential bromination, hydrolysis of bromomethyl groups affording dialdehyde, followed by a Wittig reaction (Supporting Information, Scheme S1). The dibromo derivative **2** could be selectively monolithiated and then borylated, affording **3** as a mixture of (*E*/*Z*)-isomers in 71% yield. To simplify the structural analysis using ^{1}H NMR, the (*E*/*Z*)-mixture of **3** was isomerized into the (*E*,*E*)-isomer in the presence of a catalytic amount of bis(acetonitrile)dichloro-palladium(II) ($PdCl_2(MeCN)_2$).[52] Suzuki coupling reaction of (*E*,*E*)-**3** with 1-iodo-2-((*E*)-prop-1-enyl)benzene (**4**) provided 5-bromobiphenyl derivative **5** in 91% yield as the (*all-E*)-isomer. In ^{1}H

NMR spectrum of **5**, three doublet peaks assignable for the three olefin side groups were detected at different chemical shifts and whose *J*-coupling values were always ca. 17 Hz, suggesting that the (*all-E*)-isomer is dominant for **5**. The (*all-E*)-**5** was again lithiated and borylated, affording 3-borylbiphenyl derivative (*all-E*)-**6**. The 5-borylbiphenyl (**6**) was used for subsequent synthesis as the terminal fragment of the *m*-septiphenyl (**9**).

Scheme 1. Synthesis of Helically Twisted Analogue of Kekulene 1.[a]

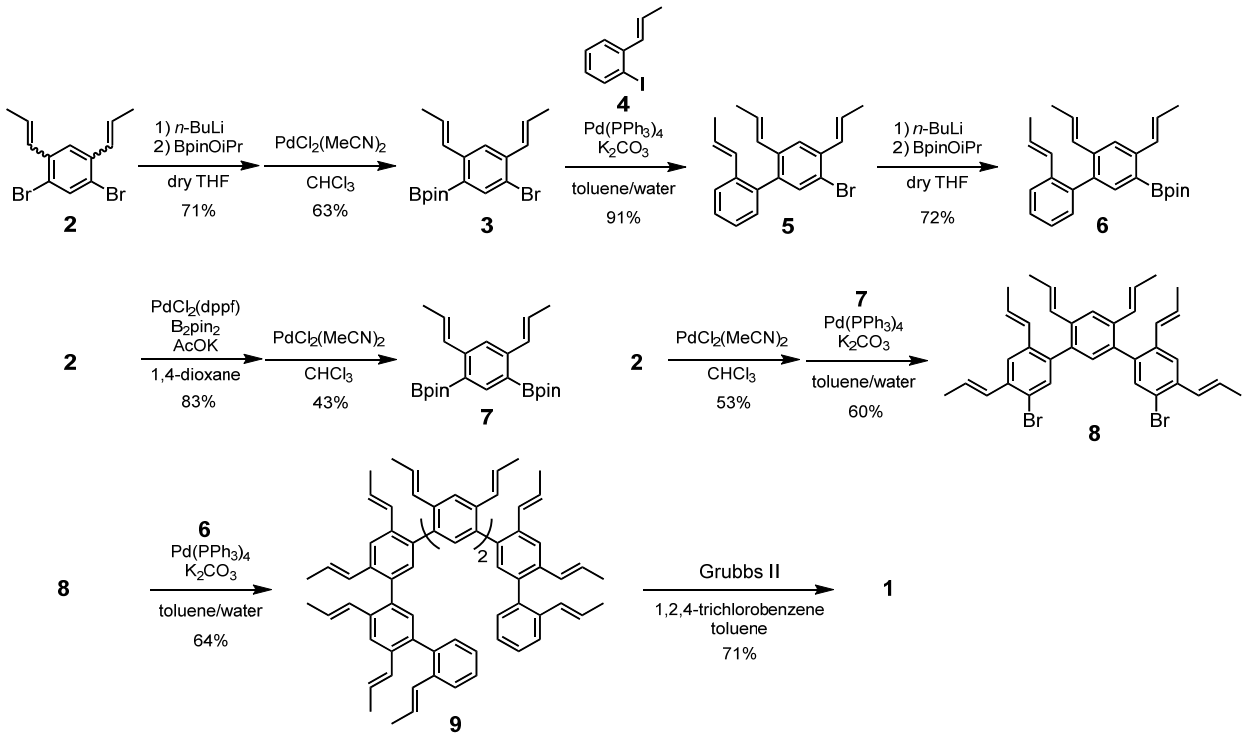

[a]B_2pin_2: bis(pinacolato)diboron; Grubbs II: Grubbs' second generation catalyst.

A 2-fold borylation reaction of **2** was satisfactory proceeded by a palladium-catalyzed borylation reaction, affording 1,5-diboryl-2,4-bis(prop-1-enyl)benzene (**7**) in 83% yield as an (*E/Z*)-mixture, which was subsequently treated with $PdCl_2(MeCN)_2$ to give (*E,E*)-**7**. Suzuki coupling reaction of (*E,E*)-**7** with an excess amount of (*E,E*)-**2** (6 mol equiv.) provided (*all-E*)-**8** in 60% yield. The key precursor *m*-septiphenyl (**9**) was then synthesized by Suzuki coupling reaction of 5,5"-dibromo-*m*-terphenyl (**8**) as the middle fragment with 2 molar equivalent of 3-borylbiphenyl (**6**) as the terminal fragment in 64% yield.

We note that totally 7 different singlet peaks were detected in the aromatic region (6.8–8.0 ppm) for ^{1}H NMR spectrum of (*all-E*)-**8**, which has more than 4 aromatic H-atoms expected from the chemical structure of **8**. This result suggested a slow rotation dynamics of the *m*-phenylene framework compared to the time scale of NMR measurement at room temperature. Indeed, the 7 peaks observed in $CDCl_3$ at 25 °C started to merge into 4 singlet peaks at 50 °C with the intensity ratio of 1:2:2:1, supporting the existence of rotation isomers for (*all-E*)-**8** (Figure S1 in the Supporting Information). Likewise, ^{1}H NMR spectrum of (*all-E*)-**9** was remarkably complicated probably due to the slow rotation dynamics of the *m*-oligophenyl with bulky olefins; there are 20 different rotamers for *m*-septiphenyl **9** expected by considering the 6 rotatable C–C single bonds (Table S1).

Finally, a 6-fold RCM reaction of **9** using Grubbs' second generation catalyst (Grubbs II) was successfully proceeded, affording helical analogue of kekulene **1** in 71% yield. The structure of **1** was fully characterized by ^{1}H NMR, ^{13}C NMR, HMQC/HMBC measurements, and high-resolution mass spectrometry (see the Supporting Information for details). In contrast to the extremely low solubility nature of kekulene[43,44] and septulene (ca. 1 mg/20 mL in 1,2,4-trichlorobenzene at 100 °C),[51] the helical analogue **1** was moderately soluble in organic solvents such as tetrahydrofuran (THF), 1,2,4-trichlorobenzene, and carbon disulfide (CS_2) (ca. 1 mg/mL in each solvent). The ^{1}H NMR of **1** (in $CS_2/CDCl_3$ = 2/1) showed characteristic three singlet peaks at 10.75, 10.71, and 10.48 ppm with the intensity ratio of 1:2:2, assignable to the inner protons of helical structure. Theoretically estimated chemical shifts for **1** were 11.47 ppm for the three inner protons of the rings E, G, and I, and 11.22 ppm for the rings C and K, calculated at the GIAO-B3LYP/6-311g(2d,p) level of theory.

Nomenclature for π-Expanded Helicenes. According to the IUPAC nomenclature, the name of **1** would be dinaphtho[1″,2″:6,7;1‴,2‴:6′,7′]diphenanthro[3,2-a:2′,3′-j]anthracene. As seen in this example, the IUPAC nomenclature tends to provide very complicated name, especially for a polycyclic system, from which it is difficult to estimate the exact molecular structure.[45] We

propose an alternative nomenclature that is helpful to provide an intuitive name for the π-expanded helicenes, based on the corannulene nomenclature proposed by Agranat.[53] In the corannulene nomenclature, like corannulene[n^m,⋯], the numbers in square brackets (n) denote the size of n-membered rings and the superscript numbers (m) designate the number of outer carbon atoms unshared by the neighboring rings. Accordingly, [7]helicene, [7]heliphene, and **1** are named helicene[6,6^2,6^2,6^2,6^2,6^2,6], helicene[6,4^0,6^2,4^0,6^2,4^0,6^2,4^0,6^2,4^0,6^2,4^0,6], and helicene[6,6^2,6^1,6^2,6^1,6^2,6^1,6^2,6^1,6^2,6^1,6^2,6], respectively. The long names can be shortened to helicene[6,$(6^2)_5$,6]), helicene[6,$(4^0,6^2)_5$,4^0,6], and helicene[6,$(6^2,6^1)_5$,6^2,6]) as a simplified form. Thus, the structure of **1**, i.e., the size and number of polycyclic rings and the connectivity consisting of the alternating angular (m = 2) and linear (m = 1) annulations, could be clearly indicated by the proposed nomenclature.

X-ray Crystallography. The π-expanded helical structure of **1** was unambiguously determined by X-ray crystallography (Figure 2). To the best of our knowledge, this is the first report of the single crystal structure of non-functionalized helical analogue of kekulene, which provides fundamental insights into molecular structure, local aromaticity, and the nature of intermolecular interactions of π-expanded helicenes. A single crystal suitable for X-ray analysis

was obtained by a slow vapor diffusion of hexane into a concentrated solution of **1** in tetrahydrofran (THF). The crystal was a racemate (monoclinic, space group *I*2/*a*) composed of 1:1 mixture of enantiomers. The two enantiomers, i.e., (*P*)-**1** and (*M*)-**1**, were alternately stacked along the *b*-axis so that the quasiplanar part of helical molecule, i.e., the seven middle rings from D to J, were overlapped each other, where the interplanar distances were alternately 3.32 and 3.35 Å (Figure 2b and 2c). For the racemic dimer pair with the shortest interplanar distance ($d_{FGH–FGH}$ = 3.32 Å), the adjacent (*P*)-**1** and (*M*)-**1** were interacted each other so that five benzenoid rings, i.e., rings from F to J, were overlapped (Figure 2c). The π-stacked racemic column structure is commonly seen in the other π-expanded helicenes, i.e., [7]heliphene by Vollhardt[36] and a selenophene-annulated expanded helicene by Tilley,[42] but not seen in the crystal structures of [7]helicene.[54] The π-stacked racemic column of **1** along the *b*-axis were arranged in a herringbone manner, where the molecular plane defined by the central three rings F, G, and H formed an angle of 29° with the vertical plane of the *b*-axis (Figure 2b). The herringbone angle (θ_{HB})—the inclination of the molecular planes in adjacent columns—was therefore 58° for **1**. Similar herringbone-type crystal packing was reported for kekulene (θ_{HB} = 86°)[44] and septulene (θ_{HB} = 55°),[51] however, it is not seen in the π-expanded helicenes reported by Vollhardt[36–38] and Tilley.[42] In this context, the crystal structure of **1** can be regarded as having both features of π-expanded

helicenes, e.g., heliphenes, and disk-shaped planar PAHs, e.g., kekulene[43,44] as well as coronene and ovalene.[55]

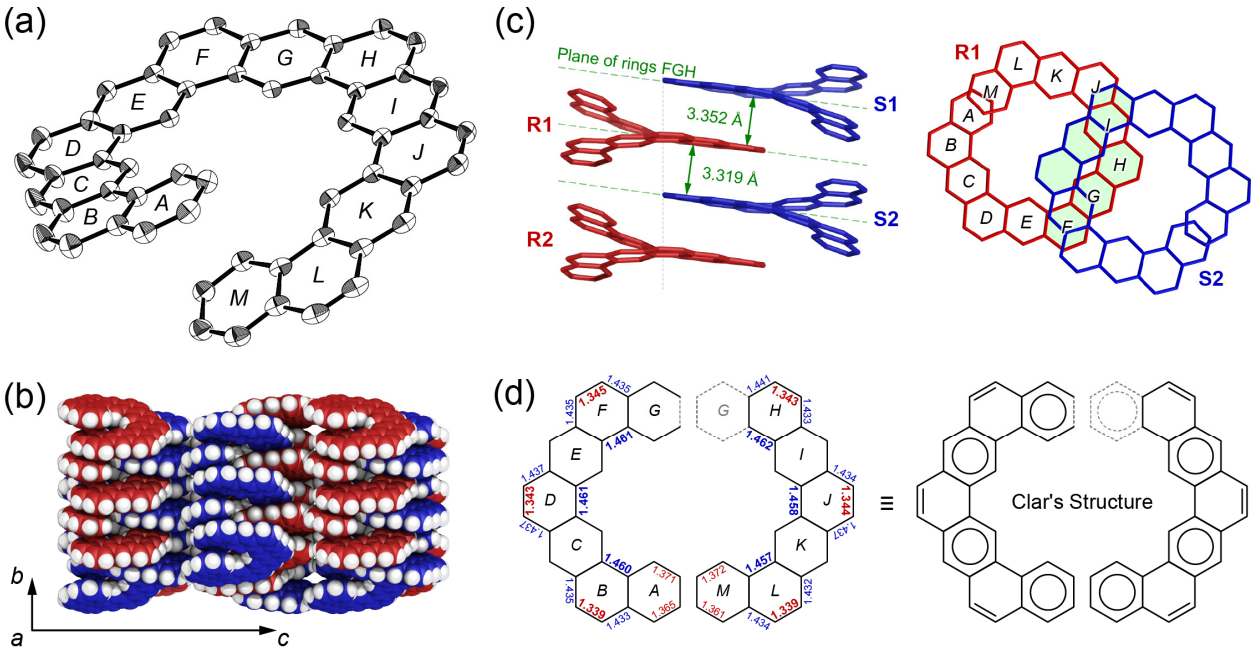

Figure 2. Crystal structure of helical analogue of kekulene **1** ($C_{54}H_{30}$). (a) ORTEP drawing of **1** recorded at 93 K, showing 50% probability thermal ellipsoids. Hydrogen atoms are omitted for clarity. (b) Crystal packing structure of **1** viewed normal to the $(\bar{1}00)$ face. (*P*)-**1** and (*M*)-**1** are colored in red and blue, respectively. Co-crystalized solvent molecules, i.e., hexane and THF, are omitted for clarity (see the Supporting Information for details). (c) Crystal packing structure of the π-stacked racemic column of **1**. Left, the side view of the racemic column, in which green dashed lines represents the least-square planes defined by the central rings F, G, and H. Right, the top view of the racemic dimer with the shortest interplanar distance of $d_{FGH–FGH}$ = 3.319 Å, viewed nomal to the plane defined by the rings F, G, and H. Five aromatic rings (i.e., rings F–J) were well overlapped each other in the closest dimer pair. (d) Bond length in angstrom of the unit determined by X-ray crystallography.

The bond length determined by X-ray crystallography provides fundamental information on the electronic structure of **1**. The representative values of bond length larger than 1.43 Å or shorter than 1.38 Å are shown in Figure 2d. Obviously, there are two types of six-membered rings in **1**. The bond lengths for the inner rim and outer edges in the even-numbered rings—i.e., the angular rings B, D, F, H, J, and L—were 1.460 ± 0.002 and 1.342 ± 0.002 Å, respectively, which are almost identical to the bond lengths of butadiene (1.47 and 1.35 Å for single- and double-bonds, respectively).[56] On the other hand, the odd-numbered rings—i.e., the terminal rings A and M, and the linearly fused rings C, E, G, I, and K—had intermediate bond lengths within the range of 1.36–1.43 Å, which was close to the typical length for aromatic rings (ca. 1.39 Å). On the basis of the bond lengths, the values of the harmonic oscillator model of aromaticity (HOMA)[57] for each type of rings were $HOMA_{even}$ = 0.39 ± 0.04 and $HOMA_{odd}$ = 0.89 ± 0.02, suggesting the olefinic character for the angular (even) rings and the benzenoid character for the terminal and linear (odd) rings. On the basis of the structural analysis, the electronic structure of **1** is best represented by the Clar's sextet notation (Figure 2d), which is fully consistent with the X-ray structures of the planar macrocyclic analogues, i.e., kekulene[44] and septulene.[51]

Local Aromaticity. The local aromaticity of helical analogue of kekulene **1** was investigated by the nucleus-independent chemical shifts (NICS)[58] calculated at the GIAO-

B3LYP/6-311g(2d,p) level. Negative NICS(0) values with strong intensity were found at the center of the odd numbered rings, i.e., A and M rings, −9.11 ppm; C and K rings, −9.24 ppm; E and I rings, −8.91 ppm; G ring, −8.94 ppm, whereas negative values with moderate intensity at the even numbered rings, i.e., B and L, −4.20 ppm; D and J, −2.37 ppm; F and H, −2.53 ppm (Supporting Information, Figure S5). The result of the calculated local aromaticity was in a good agreement with the bond length analysis based on the HOMA index; large negative NICS values were found in the rings with a large HOMA value. The alternately localized aromatic character of **1** is consistent with the planar analogues, i.e., kekulene[44] and septulene,[51] which is likely attributed to the ring connectivity consisting of the alternating angular and linear annulations.

Local Structural Deformation. A careful comparison of the X-ray structures suggested that the structural deformation of **1** is significantly smaller than that of [7]helicene (Figure 3). The vertical distances (*d*) from the centroid of the teriminal rings A and M to the least-squares plane defined by the central three ring F, G, and H were $d_{A–FGH}$ = 1.65 and $d_{M–FGH}$ = 1.66 Å for **1**. The sum of the two values was $\Sigma d_{A/M–FGH}$ = 3.31 Å, which is close to the typical π-π distance (3.4 Å). The sum of the vertical distances was about 10% larger for [7]helicene ($\Sigma d_{A/G–CDE}$ = 3.67 Å), suggesting that the helical geometry of [7]helicene is largely distorted. Difference in the helical

distortion was also suggested by the angle between the two planes (θ) defined by the terminal rings; the terminal rings of **1** arranged more parallelly (θ_{AM} = 18.2°) than those of [7]helicene (θ_{AG} = 32.8°). The local structural deformation is directly reflected to the torsion angle along the helical inner rim (ϕ). The torsion angles of **1** were ϕ = 0.9, 5.4, 3.0, 3.6, 7.5, and 7.9° along the six fjord regions from the rings ABC to rings KLM. The mean value was $<\phi_{AM}>$ = 5 ± 2° for the 6 torsion angles of **1**, which is significantly smaller than that of [7]helicene ($<\phi_{AG}>$ = 22 ± 3°). Thus, the local structural distortion of **1** was remarkably small compared to [7]helicene, likely due to the π-expanded helicene structure with large helical diameter.

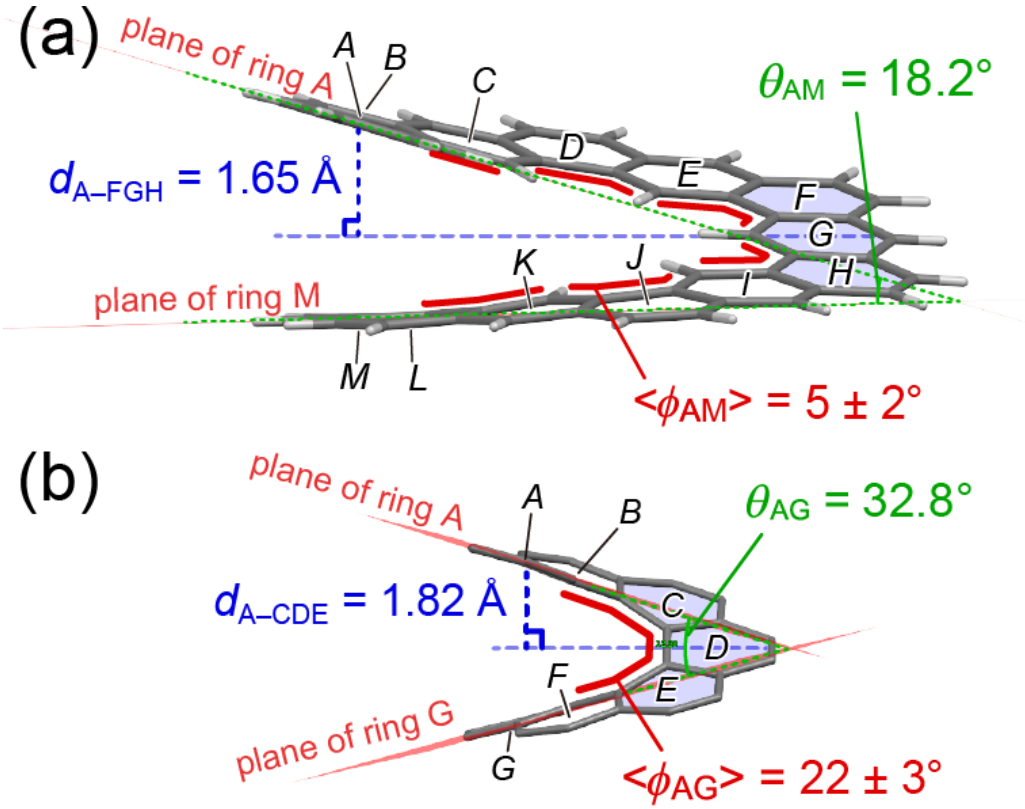

Figure 3. Comparison of crystal structures between (a) **1** and (b) [7]helicene. The angle between the two planes (θ_{AM}) of the terminal rings is highlighted in green. The torsion angle along the helical inner rim ($<\phi_{AM}>$) is highlighted in red.

UV-vis Absorption and Emission in Solution. UV-vis absorption and emission spectra of **1** was measured in chloroform (Figure 4). Compound **1** showed a strong absorption band at 320 nm ($\varepsilon = 1.4 \times 10^5$ $M^{-1}\cdot cm^{-1}$) and structured bands at 375 and 395 nm with moderate intensities ($\varepsilon = 3.5 \times 10^4$ and 3.8×10^4 $M^{-1}\cdot cm^{-1}$, respectively). Upon excitation with UV light (λ_{ex} = 320 nm), a structured emission spectrum was recorded with maximum peak wavelengths at 448, 461, 481, and 515 nm, which is commensurate with a blue emission. The absorption and fluorescence spectra of **1** were quite similar in shape to those of kekulene[43,44] and septulene[51] (Figure S7). The similarity of absorption and emission spectra in the open-ring (**1**) and the closed-ring analogues (kekulene and septulene) suggests that the contribution of the macrocyclic conjugation in the closed-ring structure, i.e., superaromaticity, to the electronic structures is almost negligible in both the ground and excited states. Thus, the experimental results of the absorption and emission spectra of non-functionalized derivative **1** is a convincing evidence supporting the theoretical result of very small superaromatic stabilization energy (SSE) for kekulene and septulene.[45,59] The fluorescence quantum yield (Φ_f) and mean fluorescence lifetime ($<\tau_f>$) of **1** were $\Phi_f = 0.04$ and $<\tau_f> = 33$ ns

(Table S7). On the basis of the two parameters, the fluorescence emission (k_f) and nonradiative decay rate constants (k_{nr}) of **1** were determined at $k_f = 0.001$ ns^{-1} and $k_{nr} = 0.03$ ns^{-1}, respectively, which are comparable to those of [7]helicene in chloroform (Φ_f, 0.04; $<\tau_f>$, 26 ns; k_f, 0.002 ns^{-1}; k_{nr}, 0.04 ns^{-1}).[60]

Experimentally observed absorption spectrum of **1** was well reproduced by time-dependent density functional theory (TD-DFT) calculations at the B3LYP/6-311g(2d,p) level of theory (Figure 4). According to the calculations, the absorption band appeared at 395 nm was attributed to a combination of the HOMO−1 → LUMO (48%) and the HOMO → LUMO+1 (47%) transitions ($f = 0.380$, $\lambda_{max,calc} = 402$ nm). The strong absorption band appeared at 320 nm was attributed to a symmetry allowed transition ($f = 1.250$, $\lambda_{max,calc} = 327$ nm) corresponded to the S_0–S_{18} transition consisting of complicated contributions of many transitions including the HOMO → LUMO+3 (28%), the HOMO−3 → LUMO (19%), and the HOMO−1 → LUMO+2 (15%) transitions.

Designing a large transition magnetic dipole moment (TMDM) of electronic transitions is crucial to create chiral molecules with an excellent chiroptical properties.[61] The dissymmetry factor (g), that is a measure of the selective response of chiral molecules to the left and right circularly polarized light (CPL), can be expressed as follows; $g = 4R/(D + G) = 4(|\boldsymbol{\mu}|\cdot|\boldsymbol{m}|\cdot\cos\theta)/(|\boldsymbol{\mu}|^2$

+ $|\boldsymbol{m}|^2$), where R, D, and G represent the rotatory, electric dipole, and magnetic dipole strengths, respectively, $\boldsymbol{\mu}$ and $\boldsymbol{m}$ transition electric dipole moment (TEDM) and TMDM, respectively, and θ the angle of TEDM and TMDM.[62,63] The g value is always zero for achiral molecules, and ideal molecules that selectively respond to only either the left- or right-handed CPL have the maximum g value (i.e., g = +2 and −2 for the left- and right-handed CPL, respectively). According to this equation, the g value takes the maximum value when the two vectors of TEDM and TMDM have the same magnitude and the directions of the two vectors are parallel (i.e., $g = \pm 2$ when $|\boldsymbol{\mu}| = |\boldsymbol{m}|$ and $\cos\theta = 1$).[64] Considering the electronic transitions of organic molecules, the magnitude of TEDM is usually several orders of magnitude larger than TMDM, therefore, the large g value can be logically designed by making the magnitude of TMDM large or making TEDM small (i.e., $g \sim (4|\boldsymbol{m}|/|\boldsymbol{\mu}|)$ when $|\boldsymbol{\mu}| >> |\boldsymbol{m}|$ and $\cos\theta = 1$). The magnitude of TEDM can be well controlled by molecular design in intuitive manner because TEDM is approximately proportional to the root of oscillator strength (f), however, no clear relationship between the molecular structure and the magnitude of TMDM has not been established yet.

Interestingly, TD-DFT calculations suggested that the transition magnetic dipole moment (TMDM) of π-expanded helicene **1** was significantly larger than the other helical molecules; the magnitude of TMDM was $|\boldsymbol{m}|$ = 3.149, 4.800, and 9.039 erg·Gauss^{-1} for [7]helicene, [7]heliphene,

and **1**, respectively (Table 1). For the corresponding planar PAHs, the TMDM became large in a similar manner as increasing the diameter of macrocyclic structures; $|\boldsymbol{m}|$ = 3.669, 5.542, and 9.918 erg·Gauss^{-1} for coronene, anti-kekulene, and, kekulene, respectively. From these results, the large TMDM observed for π-expanded helicene **1** is likely attributed to the large helical diameter. In this context, the pure enantiomers of the π-expanded helicene, i.e., (*P*)-**1** and (*M*)-**1**, are expected to show an excellent chiroptical properties because of the large TMDM. For the investigation of circular dichroism (CD) and circularly polarized luminescence (CPL), we tried to isolate the enantiomers of **1** using chiral HPLC, however, no separation was detected under any condition tested.

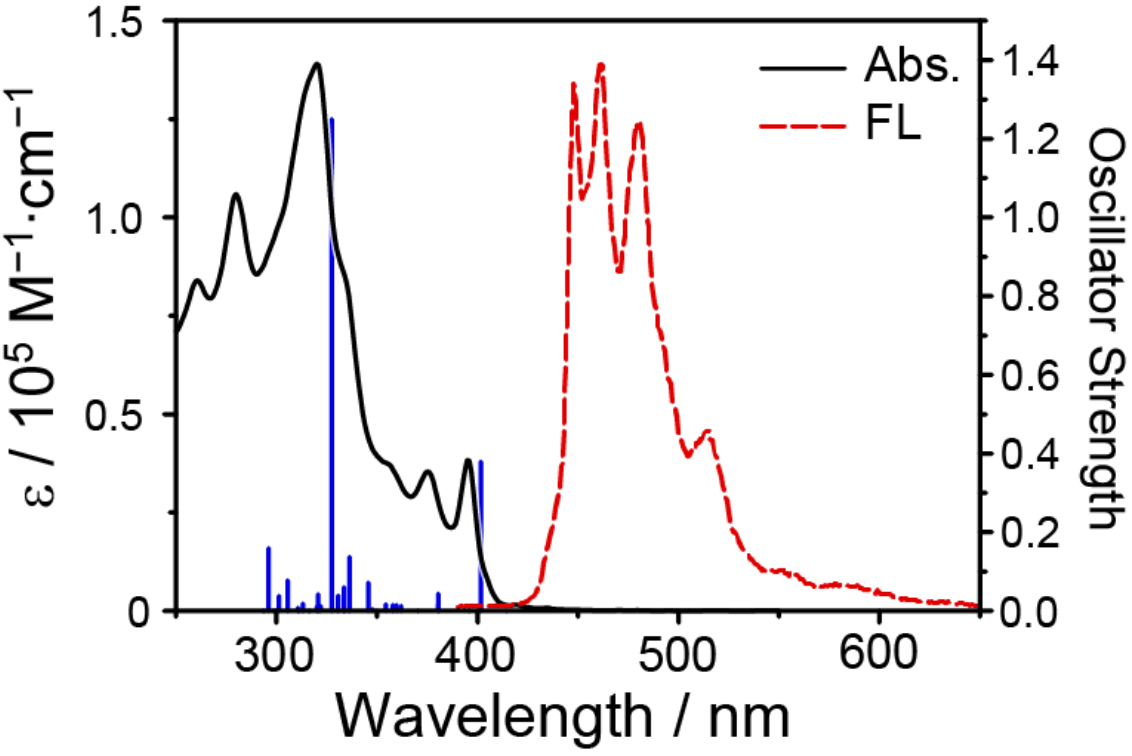

Figure 4. Absorption (black solid line) and fluorescence (red dashed line) spectra of **1** in chloroform ($c = 7 \times 10^{-7}$ M, $\lambda_{ex} = 320$ nm). Blue bar represents the oscillator strengths of electronic transitions of **1** calculated at the TD-B3LYP/6-311g(2d,p) level of theory.

Table 1. Transition dipole moments and chiroptical properties of planar and helical PAHs.[a]

Compd	$\lvert\boldsymbol{\mu}\rvert$ [b] / 10^{-20} esu·cm	$\lvert\boldsymbol{m}\rvert$ [c] / 10^{-20} erg·Gauss^{-1}	$\cos(\theta_{\mu,m})$ [d]	$\lvert g\rvert$ [e]
coronene	0.00	3.669	–	–
anti-kekulene	0.00	5.542	–	–
kekulene	0.00	9.918	–	–
[7]helicene	290.02	3.149	0.681	0.0296
[7]heliphene	298.33	4.800	0.469	0.0302
1	569.80	9.039	0.419	0.0266

[a] Calculated at the TD-B3LYP/6-311g(2d,p) level of theory. The electronic transition having large transition magnetic dipole moment ($\lvert\boldsymbol{m}\rvert$) was chosen in this table (See the Supporting Information) i.e., The values of the S_0–S_1 transition for anti-kekulene and [7]heliphene, the S_0–S_2 transition for kekulene, the S_0–S_3 transition for [7]helicene and **1**, and the S_0–S_7 transition for coronene.

Helical Inversion Process. According to the literature,[36,37] the barrier for the helical inversion of a [7]heliphene derivative is remarkably low ($\Delta G^{\ddagger}$ = 12.6 kcal·mol^{-1} at −27 °C determined by low-temperature ^{1}H NMR study) compared to [7]helicene ($\Delta G^{\ddagger}$ = 41.7 kcal·mol^{-1}).

Vollhardt reported that the low configurational stability of [7]heliphene is likely associated with the flexible molecular framework of phenylenes that consists of alternating 6- and 4-membered rings.[38] Based on this background, the racemization dynamics of **1**, consisting solely of 6-membered benzene rings, is of primary interest in the π-expanded helicene chemistry. DFT calculations suggested that the activation barrier for the helical inversion of **1** were $\Delta G^{\ddagger}$ = 54.3 kJ·mol^{-1} (13.0 kcal·mol^{-1}) at 25 °C calculated at the B3LYP/6-311g(2d,p) level of theory (Figure 5). The corresponding thermodynamic parameters were determined at $\Delta H^{\ddagger}$ = 41.1 kJ·mol^{-1} and $\Delta S^{\ddagger}$ = −44.4 J·mol^{-1}·K^{-1}, from which the half-life of the helical inversion process of **1** was estimated to be only $\tau_{1/2}$ = 0.4 ms at 25 °C (Tables 2 and S9). To compare the $\Delta G^{\ddagger}$ value with the other reference molecules, the activation barriers were also calculated for [7]heliphene and [7]helicene in the same conditions, which were $\Delta G^{\ddagger}$ = 74.3 and 170.0 kJ·mol^{-1} (17.7 and 40.6 kcal·mol^{-1}), respectively. Thus, the racemization barrier of **1** was suggested to be even smaller than that of [7]heliphene (Figure S14). We note that there was no configurational disorder between (*P*)-**1** and (*M*)-**1** in the single crystalline structure (Figure 2), suggesting that the helical inversion process of **1** can be well suppressed in the solid state or in the rigid matrixes.

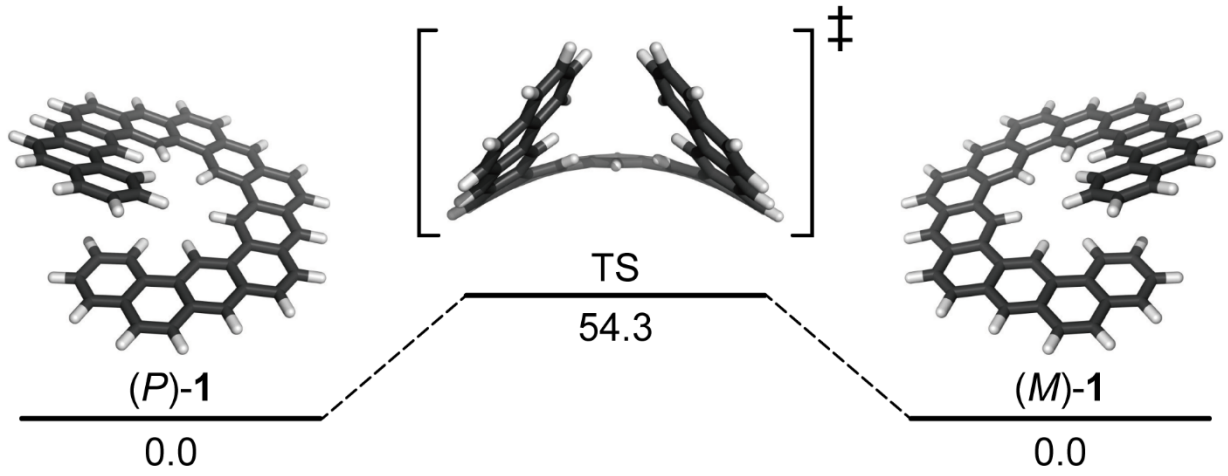

Figure 5. Racemization process between (*P*)-**1** and (*M*)-**1** and the relative Gibbs free energy (kJ·mol−1) calculated at the B3LYP/6-311g(2d,p) level of theory.

Table 2. Thermodynamic parameters for the helical inversion process.[a]

compd	$\Delta H^{\ddagger}$ / kJ·mol^{-1} (kcal·mol^{-1})	$\Delta S^{\ddagger}$ / J·mol^{-1}·K^{-1} (cal·mol^{-1}·K^{-1})	$\Delta G^{\ddagger}$ / kJ·mol^{-1} (kcal·mol^{-1})		
			−50 °C	25 °C	100 °C
1	41.1 (9.8)	−44.4 (−10.6)	51.0 (12.2)	54.3 (13.0)	57.7 (13.8)
[7]heliphene	67.7 (16.2)	−21.9 (−5.2)	72.6 (17.4)	74.3 (17.7)	75.9 (18.1)
[7]helicene	165.0 (39.4)	−16.7 (−4.0)	168.7 (40.3)	170.0 (40.6)	171.2 (40.9)

[a] Calculated at the B3LYP/6-311g(2d,p) level of theory.

Molecular Spring Constants. Flexibility of molecular framework was investigated based on the change of the potential energy (E_{el}) upon elongation of molecular springs (Figure 6). The distance between the two carbon atoms at the end of molecule (r) in equilibrium structure was 5.15, 5.33, and 5.59 Å for **1**, [7]heliphene, and [7]helicene, respectively. The potential energy

surface was scanned from the equilibrium structure with 10 steps in 0.2 Å increments. By fitting the change of potential energy using the function of spring energy, i.e., $\Delta E_{el} = (1/2)\cdot k\cdot(\Delta r)^2$, the force constants ($k$) of the molecular springs was determined as k = 0.33, 0.86, and 3.07 $N\cdot m^{-1}$ for **1**, [7]heliphene, and [7]helicene, respectively. It is noted that the force constant of **1** (0.33 $N\cdot m^{-1}$) was almost one-tenth of [7]helicene (3.07 $N\cdot m^{-1}$) and less than half of [7]heliphene (0.86 $N\cdot m^{-1}$), suggesting that the π-expanded helicene **1** can be regarded as a soft molecular spring with a small spring constant. Interestingly, the intensity ratio of the force constants of molecular spring, (1/2.6/9.3 for **1**/[7]heliphene/[7]helicene), roughly satisfied the force constant formula of macroscopic spring materials—i.e., the spring constant is inversely proportional to the third power of the diameter ($k \propto d_h^{-3}$); the force constant ratio of 1/2/8 was expected from the helical diameter of molecules (d_h = 10.2/8.2/5.1 Å) according to the force constant formula.[65]

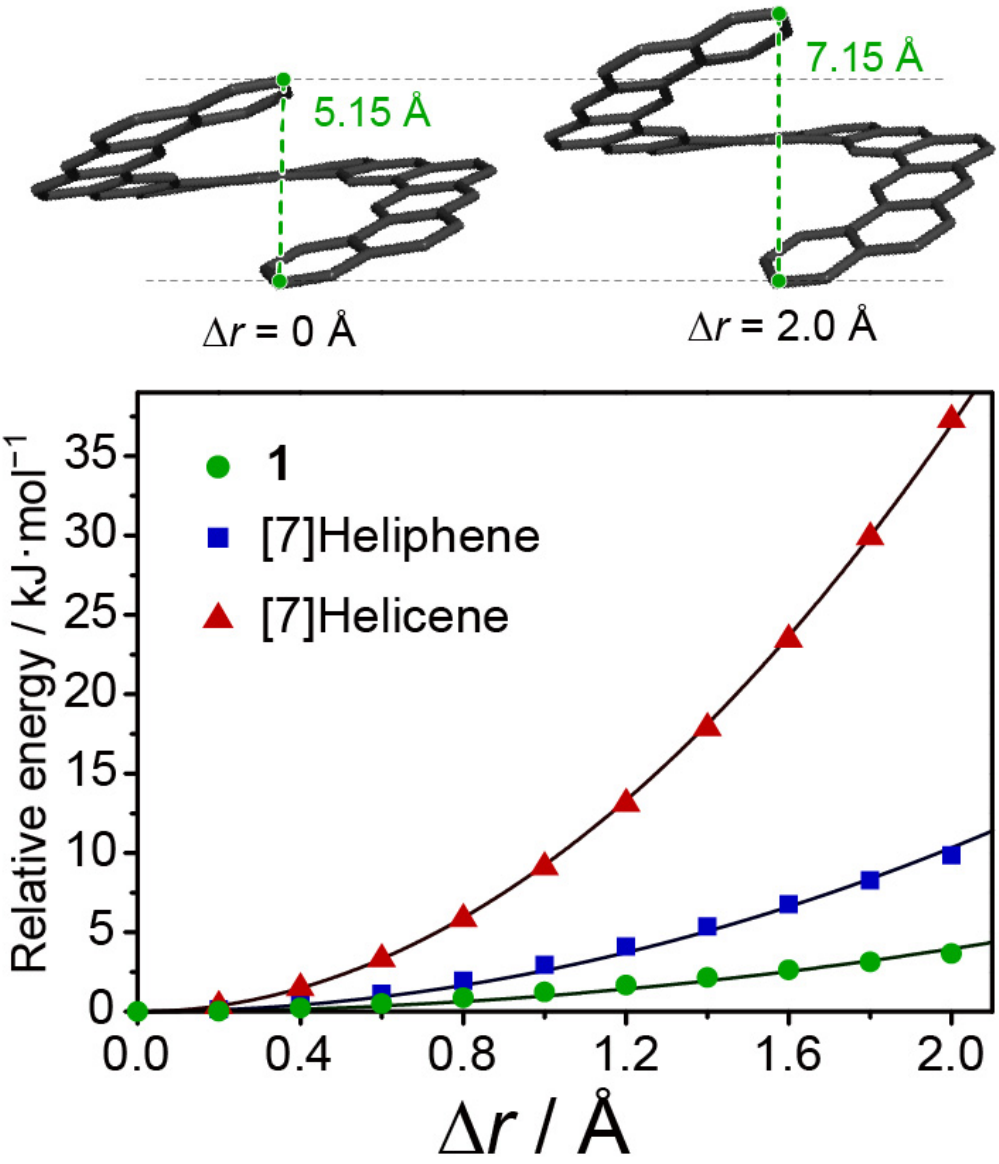

Figure 6. Increase of energy upon elongation of molecular spring of helical analogue of kekulene **1** (green circle), [7]heliphene (blue square), and [7]helicene (red triangle) calculated at the B3LYP/6-311g(2d,p) level of theory.

Conclusion

In conclusion, a π-expanded helicene (**1**)—that is the helically twisted analogue of kekulene—was successfully synthesized using a ring-closing olefin metathesis reaction. The electronic state of **1** was very similar to the cyclic planar PAH analogues, i.e., kekulene and septulene, as evidenced by the alternately localized aromatic character and the absorption and emission properties of **1**. We found that the transition magnetic dipole moment of **1** was approximately three times larger than that of [7]helicene, which is likely attributed to the π-expanded molecular geometry with the large helical diameter. Associated with the small local deformation, the activation barrier for the helical inversion significantly decreased with increasing the helical diameter of helix-shaped molecules. The flexibility of the π-expanded helicene framework is likely attributed to the number of C–C bonds in a helical pitch, which appears to be a similar origin of the mechanical properties of the macroscopic spring materials. Since the π-expanded helicene having a larger helical diameter is consisting of more C–C bonds per helical pitch, the steric distortion required for the elongation of molecular spring can be effectively distributed throughout the molecular structure. From this perspective, π-expanded helicenes are promising candidates for molecular springs with a small spring constant. Synthetic strategy to extend the π-expanded helicene framework along the helical axis and the elucidation of unique

chiroptical properties of the helical analogue of kekulenes are currently under investigation in our group.

Experimental Section

Synthesis of 2,2′′′′′′,4′,4′′,4′′′,4′′′′,4′′′′′,6′,6′′,6′′′,6′′′′,6′′′′′-hexadeca((*E*)-prop-1-enyl)-*m*-septiphenyl (9). To a solution of (*all-E*)-**8** (64 mg, 0.10 mmol), (*all-E*)-**6** (88 mg, 0.22 mmol), and K_2CO_3 (90 mg, 0.65 mmol) in toluene (4 mL) and water (1.5 mL) was added $Pd(PPh_3)_4$ (40 mg. 0.035 mmol) under N_2 atmosphere. The reaction mixture was stirred at 100 °C for 17 h. After cooling to room temperature, the reaction mixture was washed with water and extracted with CH_2Cl_2. The combined organic layer was dried over $MgSO_4$, filtered, and evaporated to dryness. The crude product was purified by silica gel column chromatography (hexane/CH_2Cl_2 = 85/15) to give (*all-E*)-**9** (66 mg, 0.065 mmol, 64%) as a white solid. ^{1}H NMR (500 MHz, $CDCl_3$, δ): 1.53–1.91 (m, 36H), 5.98–6.38 (m, 24H), 6.80–7.38 (m, 11H), 7.48–7.59 (m, 2H), 7.64–7.78 (m, 5H); HRMS–APCI–Orbitrap (*m*/*z*): $[M + H]^+$ calcd for $C_{78}H_{79}^+$, 1015.6176; found, 1015.6155.

Synthesis of Dinaphtho[1′′,2′′:6,7;1′′′,2′′′:6′,7′]diphenanthro[3,2-a:2′,3′-j]anthracene (1). A solution of (*all-E*)-**9** (36 mg, 0.035 mmol) and 2,6-dichloro-1,4-benzoquinone (10 mg, 0.057 mmol) in 1,2,4-trichlorobenzene (2.5 mL) and toluene (2.5 mL) was degassed by

Freeze-Pump-Thaw cycles four times. Grubbs 2nd generation catalyst (14 mg, 0.016 mmol) was then added under N_2 atmosphere and the reaction mixture was stirred at 70 °C for 3 days. After cooling to room temperature, $CHCl_3$ (6 mL) and MeOH (6 mL) were added to the reaction mixture. The resulting precipitates were filtered by suction, washed with $CHCl_3$ (20 mL) and hexane (60 mL), and dried under reduced pressure to give **1** (17 mg, 0.025 mmol, 71%) as a yellow solid. ^{1}H NMR (600 MHz, $CS_2/CDCl_3$ = 67:33, δ): 6.34 (t, *J* = 7.4 Hz, 2H), 6.71 (t, *J* = 7.3 Hz, 2H), 7.44 (d, *J* = 7.4 Hz, 2H), 7.65 (d, *J* = 8.8 Hz, 2H), 7.88 (d, *J* = 8.8 Hz, 2H), 7.90-7.96 (m, 8H), 8.406 (s, 2H), 8.410 (s, 2H), 8.42 (s, 1H), 8.79 (d, *J* = 8.0 Hz, 2H), 10.48 (s, 2H), 10.71 (s, 2H), 10.75 (s, 1H); ^{13}C NMR (151 MHz, $CS_2/CDCl_3$ = 67:33, δ): 116.1 (CH), 117.1 (CH), 117.2 (CH), 122.6 (CH), 126.2 (CH), 126.3 (CH), 127.2 (CH), 127.4 (CH), 127.5 (CH), 127.6 (CH), 127.7 (CH), 127.9 (CH), 128.0 (CH), 128.2 (4°), 129.3 (4°), 129.4 (4°), 129.8 (4°), 130.9 (4°), 131.0 (4°), 131.2 (4°), 131.5 (4°); HRMS–APCI–Orbitrap (*m*/*z*): $[M + H]^+$ calcd for $C_{54}H_{31}^+$, 679.2420; found, 679.2409.

X-ray Crystallography. X-ray crystallographic analysis was performed on a Rigaku XtaLab P200 diffractometer equipped with a Dectoris PILATUS 200 K detector, using a VariMax Mo Optic with Mo−Kα radiation (λ = 0.71075 Å) and a confocal monochromator. The data collection and cell refinement were performed using CrysAlisPro software. The structures were

solved by direct methods (SIR-2014) and refined by a full-matrix least-squares techniques against F^2 (SHELXL-2014). The all non-hydrogen atoms were refined anisotropically except for co-crystallized solvent molecules. Hydrogen atoms were placed using AFIX instructions. CCDC 1857976 contains the supplementary crystallographic data of **1**, which is available from The Cambridge Crystallographic Data Centre via www.ccdc.cam.ac.uk/data_request/cif.

Theoretical Calculations. The geometrical optimization was carried out at the B3LYP/6-311g(2d,p) level of theory implemented on Gaussian 16 package. Convergence at a local minimum structure was confirmed by no imaginary frequencies on frequency analysis. NICS(0) and NICS(1) values were calculated at the GIAO-B3LYP/6-311g(2d,p) level of theory. For NICS(1) calculations, the ghost atoms (Bq) were located at the distance of 1 Å from the least-squares plane defined by the six carbon atoms composing a hexagonal ring structure. The anisotropy of current-induced density (ACID) was calculated at the CSGT-B3LYP/6-311g(2d,p) level of theory using the Gaussian 16 package (specified by the keywords of "nmr=CSGT" and "IOp(10/93=1)") and the AICD 2.0.1 program provided by Prof. Rainer Herges (Institut für Organische Chemie, Universität Kiel).

Associated Content

Supporting Information. Experimental procedures, details of the X-ray single crystal analyses, theoretical calculations, as well as ^{1}H and ^{13}C NMR spectra. This material is available free of charge via the Internet at http://pubs.acs.org.

Author Information

Corresponding Author

*Email: thirose@sbchem.kyoto-u.ac.jp

*Email: kmatsuda@sbchem.kyoto-u.ac.jp

Notes

The authors declare no competing financial interests.

Acknowledgements

This work was supported by a Grant-in-Aid for Scientific Research on Innovative Areas "Photosynergetics" (JSPS KAKENHI Grant Number JP26107008) from MEXT, Japan. T. H. acknowledges JSPS for a Grant-in-Aid for Scientific Research (C) (JSPS KAKENHI Grant Number JP18K05077). We thank Ms. Nanae Shimanaka and Dr. Nobuhiko Hosono (Institute for

Integrated Cell-Material Sciences (iCeMS), Kyoto University Institute for Advanced Study) for the measurement of single-crystal X-ray diffraction.

References

(1) Hembury, G. A.; Borovkov, V. V.; Inoue, Y. Chirality-Sensing Supramolecular Systems. *Chem. Rev.* **2008**, *108*, 1–73.

(2) Palmans, A. R. A.; Meijer, E. W. Amplification of Chirality in Dynamic Supramolecular Aggregates. *Angew. Chem. Int. Ed.* **2007**, *46*, 8948–8968.

(3) Mateos-Timoneda, M. A.; Crego-Calama, M.; Reinhoudt, D. N. Supramolecular Chirality of Self-Assembled Systems in Solution. *Chem. Soc. Rev.* **2004**, *33*, 363–372.

(4) Noyori, R.; Ohkuma, T. Asymmetric Catalysis by Architectural and Functional Molecular Engineering: Practical Chemo- and Stereoselective Hydrogenation of Ketones. *Angew. Chem. Int. Ed.* **2001**, *40*, 40–73.

(5) Shen, Y.; Chen, C.-F. Helicenes: Synthesis and Applications. *Chem. Rev.* **2012**, *112*, 1463–1535.

(6) Mori, K.; Murase, T.; Fujita, M. One-Step Synthesis of [16]Helicene. *Angew. Chem. Int. Ed.* **2015**, *54*, 6847–6851.

(7) Šámal, M.; Chercheja, S.; Rybáček, J.; Chocholoušová, J. V.; Vacek, J.; Bednárová, L.; Šaman, D.; Stará, I. G.; Starý, I. An Ultimate Stereocontrol in Asymmetric Synthesis of Optically Pure Fully Aromatic Helicenes. *J. Am. Chem. Soc.* **2015**, *137*, 8469–8474.

(8) Gingras, M.; Félix, G.; Peresutti, R. One Hundred Years of Helicene Chemistry. Part 2: Stereoselective Syntheses and Chiral Separations of Carbohelicenes. *Chem. Soc. Rev.* **2013**, *42*, 1007–1050.

(9) Urbano, A. Recent Developments in the Synthesis of Helicene-Like Molecules. *Angew. Chem. Int. Ed.* **2003**, *42*, 3986–3989.

(10) Tanaka, H.; Inoue, Y.; Mori, T. Circularly Polarized Luminescence and Circular Dichroisms in Small Organic Molecules: Correlation between Excitation and Emission Disymmetry Factors. *ChemPhotoChem* **2018**, *2*, 386–402.

(11) Otani, T.; Tsuyuki, A.; Iwachi, T.; Someya, S.; Tateno, K.; Kawai, H.; Saito, T.; Kanyiva, K. S.; Shibata, T. Facile Two-Step Synthesis of 1,10-Phenanthroline-Derived Polyaza[7]helicenes with High Fluorescence and CPL Efficiency. *Angew. Chem. Int. Ed.* **2017**, *56*, 3906–3910.

(12) Sánchez-Carnerero, E. M.; Agarrabeitia, A. R.; Moreno, F.; Maroto, B. L.; Muller, G.; Ortiz, M. J.; de la Moya, S. Circularly Polarized Luminescence from Simple Organic Molecules. *Chem. Eur. J.* **2015**, *21*, 13488–13500.

(13) Grimme, S.; Harren, J.; Sobanski, A.; Vögtle, F. Structure/Chiroptics Relationships of Planar Chiral and Helical Molecules. *Eur. J. Org. Chem.* **1998**, 1491–1509.

(14) Botek, E.; Champagne, B.; Turki, M.; André, J.-M. Theoretical Study of the Second-Order Nonlinear Optical Properties of [*N*]Helicenes and [*N*]Phenylenes. *J. Chem. Phys.* **2004**, *120*, 2042–2048.

(15) Fox, J. M.; Katz, T. J.; Van Elshocht, S.; Verbiest, T.; Kauranen, M.; Persoons, A.; Thongpanchang, T.; Krauss, T.; Brus, L. Synthesis, Self-Assembly, and Nonlinear Optical Properties of Conjugated Helical Metal Phthalocyanine Derivatives. *J. Am. Chem. Soc.* **1999**, *121*, 3453–3459.

(16) Verbiest, T.; Van Elshocht, S.; Kauranen, M.; Hellemans, L.; Snauwaert, J.; Nuckolls, C.; Katz, T. J.; Persoons, A. Strong Enhancement of Nonlinear Optical Properties Through Supramolecular Chirality. *Science* **1998**, *282*, 913–915.

(17) Li, C.; Yang, Y.; Miao, Q. Recent Progress in Chemistry of Multiple Helicenes. *Chem. Asian J.* **2018**, *13*, 884–894.

(18) Fukui, N.; Osuka, A. Single and Doubly 1,2-Phenylene-Inserted Porphyrin Arch-Tape Dimers: Synthesis and Highly Contorted Structures. *Angew. Chem. Int. Ed.* **2018**, *57*, 6304–6308.

(19) Geng, X.; Donahue, J. P.; Mague, J. T.; Pascal, R. A.; Jr The Hairpin Furans: Easily Prepared Hybrids of Helicenes and Twisted Acenes. *Angew. Chem. Int. Ed.* **2015**, *54*, 13957–13960.

(20) Kawasumi, K.; Zhang, Q.; Segawa, Y.; Scott, L. T.; Itami, K. A Grossly Warped Nanographene and the Consequences of Multiple Odd-Membered-Ring Defects. *Nat. Chem.* **2013**, *5*, 739–744.

(21) Bédard, A.-C.; Vlassova, A.; Hernandez-Perez, A. C.; Bessette, A.; Hanan, G. S.; Heuft, M. A.; Collins, S. K. Synthesis, Crystal Structure and Photophysical Properties of Pyrene–Helicene Hybrids. *Chem. Eur. J.* **2013**, *19*, 16295–16302.

(22) Jančařík, A.; Rybáček, J.; Cocq, K.; Chocholoušová, J. V.; Vacek, J.; Pohl, R.; Bednárová, L.; Fiedler, P.; Císařová, I.; Stará, I. G.; Starý, I. Rapid Access to Dibenzohelicenes and their Functionalized Derivatices. *Angew. Chem. Int. Ed.* **2013**, *52*, 9970–9975.

(23) Buchta, M.; Rybáček, J.; Jančařík, A.; Kudale, A. A.; Buděšínský, M.; Chocholoušová, J. V.; Vacek, J.; Bednárová, L.; Císařová, I.; Bodwell, G. J.; Starý, I.; Stará, I. G. Chimerical Pyrene-Based [7]Helicenes as Twisted Polycondensed Aromatics. *Chem. Eur. J.* **2015**, *21*, 8910–8917.

(24) Schuster, N. J.; Sánchez, R. H.; Bukharina, D.; Kotov, N. A.; Berova, N.; Ng, F.; Steigerwald, M. L.; Nuckolls, C. A Helicene Nanoribbon with Greatly Amplified Chirality. *J. Am. Chem. Soc.* **2018**, *140*, 6235–6239.

(25) Schuster, N. J.; Paley, D. W.; Jockusch, S.; Ng, F.; Steigerwald, M. L.; Nuckolls, C. Electron Delocalization in Perylene Diimide Helicenes. *Angew. Chem. Int. Ed.* **2016**, *55*, 13519–13523.

(26) Kato, K.; Segawa, Y.; Scott, L. T.; Itami, K. A Quintuple [6]Helicene with a Corannulene Core as a C_5-Symmetric Propeller-Shaped π-System. *Angew. Chem. Int. Ed.* **2018**, *57*, 1337–1341.

(27) Fujikawa, T.; Segawa, Y.; Itami, K. Synthesis, Structures and Properties of π-Extended Double Helicene: A Combination of Planar and Nonplanar π-Systems. *J. Am. Chem. Soc.* **2015**, *137*, 7763–7768.

(28) Hu, Y.; Wang, X.-Y.; Peng, P.-X.; Wang, X.-C.; Cao, X.-Y.; Feng, X.; Müllen, K.; Narita, A. Benzo-Fused Double [7]Carbohelidene: Synthesis, Structures, and Physicochemical Properties. *Angew. Chem. Int. Ed.* **2017**, *56*, 3374–3378.

(29) Wang, X.-Y.; Wang, X.-C.; Narita, A.; Wagner, M.; Cao, X.-Y.; Feng, X.; Müllen, K. Syntehsis, Structure, and Chiroptical Properties of Double [7]Heterohelicene. *J. Am. Chem. Soc.* **2016**, *138*, 12783–12786.

(30) Hosokawa, T.; Takahashi, Y.; Matsushima, T.; Watanabe, S.; Kikkawa, S.; Azumaya, I.; Tsurusaki, A.; Kamikawa, K. Synthesis, Structures, and Properties of Hexapole Helicenes: Assembling Six [5]Helicene Substructures into Highly Twisted Aromatic Systems. *J. Am. Chem. Soc.* **2017**, *139*, 18515–18521.

(31) Berezhnaia, V.; Roy, M.; Vanthuyne, N.; Villa, M.; Naubron, J.-V.; Rodriguez, J.; Coquerel, Y.; Gingras, M. Chiral Nanographene Propeller Embedding Six Enantiomerically Stable [5]Helicene Units. *J. Am. Chem. Soc.* **2017**, *139*, 18508–18511.

(32) Zhu, Y.; Xia, Z.; Cai, Z.; Yuan, Z.; Jiang, N.; Li, T.; Wang, Y.; Guo, X.; Li, Z.; Ma, S.; Zhong, D.; Li, Y.; Wang, J. Synthesis and Characterization of Hexapole [7]Helicene, A Circularly Twisted Chiral Nanographene. *J. Am. Chem. Soc.* **2018**, *140*, 4222–4226.

(33) Nakakuki, Y.; Hirose, T.; Sotome, H.; Miyasaka, H.; Matsuda, K. Hexa-*peri*-hexabenzo[7]helicene: Homogeneously π-Extended Helicene as a Primary Substructure of Helically Twisted Chiral Graphenes. *J. Am. Chem. Soc.* **2018**, *140*, 4317–4326.

(34) Xu, F.; Yu, H.; Sadrzadeh, A.; Yakobson, B. I. Riemann Surfaces of Carbon as Graphene Nanosolenoids. *Nano Lett.* **2016**, *16*, 34–39.

(35) Avdoshenko, S. M.; Koskinen, P.; Sevinçli, H.; Popov, A. A.; Rocha, C. G. Topological Signatures in the Electronic Structure of Graphene Spirals. *Sci. Rep.* **2013**, *3*, 1632.

(36) Han, S.; Bond, A. D.; Disch, R. L.; Holmes, D.; Schulman, J. M.; Teat, S. J.; Vollhardt, K. P. C.; Whitener, G. D. Total Syntheses and Structures of Angular [6]- and [7]Phenylene: The First Helical Phenylenes (Heliphenes). *Angew. Chem. Int. Ed.* **2002**, *41*, 3223–3227.

(37) Han, S.; Anderson, D. R.; Bond, A.D.; Chu, H. V.; Disch, R. L.; Holmes, D.; Schulman, J. M.; Teat, S. J.; Vollhardt, K. P. C.; Whitener, G. D. Total Syntheses of Angular [7]-, [8]-, and [9]Phenylene by Triple Cobalt-Catalyzed Cycloisomerization: Remarkably Flexible Heliphenes. *Angew. Chem. Int. Ed.* **2002**, *41*, 3227–3230.

(38) Holmes, D.; Kumaraswamy, S.; Matzger, A. J.; Vollhardt, K. P. C. On the Nature of Nonplanarity in the [*N*]Phenylenes. *Chem. Eur. J.* **1999**, *5*, 3399–3412.

(39) Dai, W.; Petersen, J. L.; Wang, K. K. Synthesis and Structures of a Helical Diindenophenanthrene with Four Congested Phenyl Substituents an a Molecular Spiral Staircase. *Org. Lett.* **2004**, *6*, 4355–4357.

(40) Nakanishi, K.; Fukatsu, D.; Takaishi, K.; Tsuji, T.; Uenaka, K.; Kuramochi, K.; Kawabata, T.; Tsubaki, K. Oligonaphthofurans: Fan-Shaped and Three-Dimensional π-Compounds. *J. Am. Chem. Soc.* **2014**, *136*, 7101–7109.

(41) Nejedlý, J.; Šámal, M.; Rybáček, J.; Tobrmanová, M.; Szydlo, F.; Coudret, C.; Neumeier, M.; Vacek, J.; Chocholoušová, J. V.; Buděšínský, M.; Šaman, D.; Bednárová, L.; Sieger, L.; Stará, I. G.; Starý, I. Synthesis of Long Oxahelicenes by Polycyclization in a Flow Reactor. *Angew. Chem. Int. Ed.* **2017**, *56*, 5839–5843.

(42) Kiel, G. R.; Patel, S. C.; Smith, P. W.; Levine, D. S.; Tilley, T. D. Expanded Helicenes: A General Synthetic Strategy and Remarkable Supramolecular and Solid-State Behavior. *J. Am. Chem. Soc.* **2017**, *139*, 18456–18459.

(43) Diederich, F.; Staab, H. A. Benzenoid versus Annulenoid Aromaticity: Synthesis and Properties of Kekulene. *Angew. Chem. Int. Ed. Engl.* **1978**, *17*, 372–374.

(44) Krieger, C.; Diederich, F.; Schweitzer, D.; Staab, H. A. Molecular Structure and Spectroscopic Properties of Kekulene. *Angew. Chem. Int. Ed.* **1979**, *18*, 699–701.

(45) Miyoshi, H.; Nobusue, S.; Shimizu, A.; Tobe, Y. Non-Alternant Non-Benzenoid Kekulenes: the Birth of a New Kekulene Family. *Chem. Soc. Rev.* **2015**, *44*, 6560–6577.

(46) Diercks, R.; Vollhardt, K. P. C. Novel Synthesis of the Angular [3]Phenylene (Terphenylene) by Cobalt-Catalyzed Cyclization of Bis(2-ethynylphenyl)ethyne: a Molecule with an Internal Cyclohexatriene Ring. *Angew. Chem. Int. Ed. Engl.* **1986**, *25*, 266–268.

(47) Bell, T. W.; Jousselin, H. Expanded Heterohelicenes: Molecular Coils That Form Chiral Complexes. *J. Am. Chem. Soc.* **1991**, *113*, 6283–6284.

(48) Ogba, O. M.; Warner, N. C.; O'Leary, D. J.; Grubbs, R. H. Recent Advances in Ruthenium-Based Olefin Metathesis. *Chem. Soc. Rev.* **2018**, *47*, 4510–4544.

(49) Luliano, A.; Piccioli, P.; Fabbri, D. Ring-Closing Olefin Metathesis of 2,2'-Divinylbiphenyls: A Novel and General Approach to Phenanthrenes. *Org. Lett.* **2004**, *6*, 3711–3714.

(50) Collins, S. K.; Grandbois, A.; Vachon, M. P.; Côté, J. Preparation of Helicenes through Olefin Metathesis. *Angew. Chem. Int. Ed.* **2006**, *45*, 2923–2926.

(51) Kumar, B.; Viboh, R. L.; Bonifacio, M. C.; Thompson, W. B.; Buttrick, J. C.; Westlake, B. C.; Kim, M.-S.; Zoellner, R. W.; Varganov, S. A.; Mörschel, P.; Teteruk, J.; Schmidt, M. U.; King, B. T. Septulene: The Heptagonal Homologue of Kekulene. *Angew. Chem. Int. Ed.* **2012**, *51*, 12795–12800.

(52) Giles, R. G. F.; Lee Son, V. R.; Sargent, M. V. Palladium-Assisted (*Z*)–(*E*) Isomerization of Styrenes. *Aust. J. Chem.* **1990**, *43*, 777–781.

(53) Agranat, I.; Hess Jr., B. A.; Schaad, L. J. Aromaticity of Non-Alternant Annulenoannulenes and of Corannulenes. *Pure Appl. Chem.* **1980**, *52*, 1399–1407.

(54) Fuchter, M. J.; Weimar, M.; Yang, X.; Judge, D. K.; White, A. J. P. An Unusual Oxidative Rearrangement of [7]-helicene. *Tetrahedron Lett.* **2012**, *53*, 1108–1111.

(55) Stevens, B. Some Effects of Molecular Orientation on Fluorescence Emission and Energy Transfer in Crystalline Aromatic Hydrocarbons. *Spectochim. Acta* **1962**, *18*, 439–448.

(56) Craig, N. C.; Groner, P.; McKean, D. C. Equilibrium Structures for Butadiene and Ethylene: Compelling Evidence for Π-Electron Delocalization in Butadiene. *J. Phys. Chem. A* **2006**, *110*, 7461–7469.

(57) Krygowski, T. M.; Cyrański, M. K. Structural Aspects of Aromaticity. *Chem. Rev.* **2001**, *101*, 1385–1419.

(58) Chen, Z.; Wannere, C. S.; Corminboeuf, C.; Puchta, R.; Schleyer, P. v. R. Nucleus-Independent Chemical Shifts (NICS) as an Aromaticity Criterion. *Chem. Rev.* **2005**, *105*, 3842–3888.

(59) Aihara, J.-i.; Makino, M.; Ishida, T.; Dias, J. R. Analytical Study of Superaromaticity in Cycloarenes and Related Coronoid Hydrocarbons. *J. Phys. Chem. A* **2013**, *117*, 4688–4697.

(60) Kubo, H.; Hirose, T.; Matsuda, K. Control over the Emission Properties of [5]Helicenes Based on the Symmetry and Energy Levels of Their Molecular Orbitals. *Org. Lett.* **2017**, *19*, 1776–1779.

(61) Sato, S.; Yoshii, A.; Takahashi, S.; Furumi, S.; Takeuchi, M.; Isobe, H. Chiral Intertwined Spirals and Magnetic Transition Dipole Moments Dictated by Cylinder Helicity. *Proc. Natl. Acad. Sci. U. S. A.* **2017**, *114*, 13097–13101.

(62) Schellman, J. A. Circular Dichroism and Optical Rotation. *Chem. Rev.* **1975**, *75*, 323–331.

(63) Richardson, F. S.; Riehl, J. P. Circularly Polarized Luminescence Spectroscopy. *Chem. Rev.* **1977**, *77*, 773–792.

(64) Dekkers, H. P. J. M. Circularly Polarized Luminescence: A Probe for Chirality in the Excited State. In *Circular Dichroism Principles and Applications*, 2nd ed.; Berova, N.; Nakanishi, K.; Woody, R. W., Eds.; Wiley-VCH: New York, 2000; pp 185–215.

(65) Chen, X.; Zhang, S.; Dikin, D. A.; Ding, W.; Ruoff, R. S.; Pan, L.; Nakayama, Y. Mechanics of a Carbon Nanocoil. *Nano Lett.* **2003**, *3*, 1299–1304.

TOC Graphics

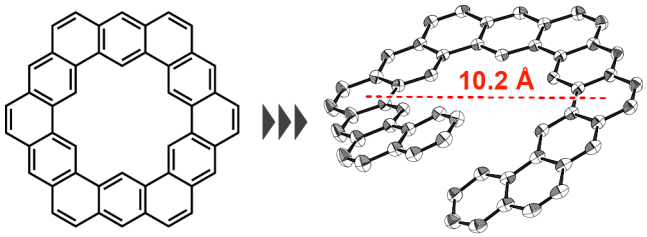

kekulene **1** ($C_{54}H_{30}$)